






Geophysical Research Letters®



RESEARCH LETTER

10.1029/2022GL100727

Spring Regional Sea Surface Temperatures as a Precursor of European Summer Heatwaves

Goratz Beobide-Arsuaga^{1,2} , André Düsterhus³ , Wolfgang A. Müller⁴ , Elizabeth A. Barnes⁵ , and Johanna Baehr¹ 

Key Points:

- A tripolar North Atlantic sea surface temperature (SST) pattern with an anomalously warm Subtropical Gyre is a precursor of European summer heatwaves
- Distinct regional spring SST anomalies relate to distinct early summer soil moisture (SM) anomaly patterns
- Distinct early summer SM anomaly patterns resemble the location of European summer heatwaves

Supporting Information:

Supporting Information may be found in the online version of this article.

Correspondence to:

G. Beobide-Arsuaga,
goratz.beobide.arsuaga@uni-hamburg.de

Citation:

Beobide-Arsuaga, G., Düsterhus, A., Müller, W. A., Barnes, E. A., & Baehr, J. (2023). Spring regional sea surface temperatures as a precursor of European summer heatwaves. *Geophysical Research Letters*, 50, e2022GL100727. <https://doi.org/10.1029/2022GL100727>

Received 19 AUG 2022
Accepted 7 JAN 2023

¹Institute of Oceanography, Center for Earth System Research and Sustainability (CEN), Universität Hamburg, Hamburg, Germany, ²International Max Planck Research School on Earth System Modelling, Hamburg, Germany, ³Department of Geography, Maynooth University, ICARUS, Maynooth, Ireland, ⁴Max Planck Institute for Meteorology, Ocean in the Earth System, Hamburg, Germany, ⁵Department of Atmospheric Science, Colorado State University, Fort Collins, CO, USA

Abstract Different spring and early summer North Atlantic sea surface temperature anomalies (SSTAs) have been shown to precede recent European summer heatwaves (EuSHWs). So far, the limited number of observed events associated with several physical mechanisms has prevented a robust identification of SSTAs as precursors. Here, we extend beyond previous studies by combining 100 historical simulations (1850–2005) of the MPI Grand-Ensemble with an explainable neural-network method. We find that the spring tripolar North Atlantic pattern with positive SSTAs in the Subtropical Gyre is a precursor of EuSHWs. In addition, positive SSTAs west of the Iberian Peninsula, and in the North Sea, the Baltic Sea and the Mediterranean Sea relate to distinct early summer soil moisture anomaly patterns and are precursors of western and southeastern EuSHWs, respectively. While the phase of the tripolar North Atlantic pattern indicates whether a EuSHW might emerge, regional SSTAs indicate the spatial characteristics of EuSHWs.

Plain Language Summary Past studies have investigated the influence of spring and early summer North Atlantic sea surface temperature anomalies (SSTAs) on recent European summer heatwaves (EuSHWs). These studies have proposed different SSTAs in the North Atlantic as the most important for the development of different EuSHWs. Yet, it has not been possible to generalize which spring North Atlantic SSTAs are the most important to anticipate EuSHWs because we have too few observed events and they showed different spatial and physical characteristics. Here, we analyze 100 historical simulations (1850–2005) of the MPI Grand-Ensemble in which we identify a large number of EuSHWs. We use an explainable neural-network method to find which spring North Atlantic SSTAs are the most important to anticipate EuSHWs. We find that warm SSTAs in the Subtropical Gyre surrounded by cold SSTAs in the north and in the south is an indicator of EuSHW occurrence. In addition, different regional SSTAs relate to drier than normal soil moisture in different parts of Europe that influence different EuSHWs. Warm SSTAs west of the Iberian Peninsula, and in the North Sea, the Baltic Sea and the Mediterranean Sea indicate the occurrence of western and southeastern EuSHWs, respectively.

1. Introduction

The large-scale oceanic and atmospheric dynamics in the North Atlantic are thermally coupled on an interannual timescale (Bjerknes, 1964; Watanabe & Kimoto, 2000). Furthermore, the coupling also occurs on a seasonal timescale. While the winter North Atlantic Oscillation (NAO) acts as a main driver imprinting spring tripolar North Atlantic sea surface temperature anomalies (SSTA), persistent SSTAs in-turn affect the atmospheric flow and can potentially precondition European summer heatwaves (EuSHWs) (Czaja & Frankignoul, 2002; Ossó et al., 2018). The tripolar SSTA pattern has been related to anticyclonic anomalies over Europe (Gastineau & Frankignoul, 2015), increasing the temperatures and decreasing precipitation by compressing the downward moving air, and blocking the westerlies and the intrusion of storm track (Rex, 1950; Treidl et al., 1981). In the case of long-lasting blocking, the soil moisture (SM) in the region decreases, reducing the latent cooling in the atmosphere and further increasing air temperatures (Fischer et al., 2007; Seneviratne et al., 2006).

The SSTAs in the Subpolar Gyre (SPG) and tropical Atlantic, both part of the tripolar North Atlantic pattern, have been related to the 2015 EuSHW (Duchez et al., 2016; Wulff et al., 2017). Duchez et al. (2016) suggested that the negative SSTAs in the SPG were responsible for the southward shift of the Jet Stream, which enhanced the

© 2023. The Authors.

This is an open access article under the terms of the [Creative Commons Attribution License](https://creativecommons.org/licenses/by/4.0/), which permits use, distribution and reproduction in any medium, provided the original work is properly cited.

blocking anticyclone over Central Europe and lead to the 2015 EuSHW. In contrast, Wulff et al. (2017) proposed that the negative SSTAs in the tropical Atlantic, and the respective diabatic heating anomalies, were responsible for the blocking system and hence, the 2015 EuSHW.

In addition to North Atlantic SSTAs, surface temperatures in different European regional seas have also been proposed to precede EuSHWs. According to Feudale and Shukla (2011), positive SSTAs in the North Sea reduced the meridional temperature gradient and baroclinic activity, allowing the blocking to persist over Europe during the 2003 EuSHW. The dominant descending motion prevented convection and increased temperatures warming the Mediterranean Sea. Positive SSTAs in the Mediterranean Sea have been related to dry and warm European summers, and are thought to be responsible for half of the amplitude of the 2003 EuSHW (Feudale & Shukla, 2007; Ionita et al., 2017).

The limited number of observed EuSHW events associated with a variety of physical mechanisms has prevented the systematic identification of SSTAs as precursors of EuSHWs. The MPI Grand-Ensemble (MPI-GE) data set combined with a neural-network (NN) based explainable artificial intelligence method, layerwise relevance propagation (LRP) (Bach et al., 2015; Toms et al., 2020), provides a unique opportunity for a systematic analysis of EuSHW precursors. Here, we robustly identify the most important spring North Atlantic SSTAs as precursors of different EuSHWs.

2. Data and Methods

2.1. Data

We use the 100-member MPI-GE with historical anthropogenic and natural forcing (1850–2005), and high temporal resolution (Maher et al., 2019). The 100 ensemble members use the same model set-up and forcing, but are started from different initial conditions all taken from the quasi-equilibrated control-run (Maher et al., 2019). MPI-GE includes the land component JSBACH with a five-layer scheme improving the representation of soil hydrological processes (Hagemann & Stacke, 2015). The MPI-GE uses the low resolution version of the MPI-ESM model, which represents well the observed connection between spring North Atlantic SSTA and Eurasian surface temperatures via atmospheric wave trains, as well as the observed frequency and amplitude of extreme European summer temperatures (Chen et al., 2021; Suarez-Gutierrez et al., 2018).

We analyze the following climate variables: daily surface maximum temperature (T2max) and monthly sea surface temperature (SST), total precipitation (TP), geopotential height at 500 hPa (Z500) and SM. SM is here defined as the fraction of water accumulated in the root zone relative to the water capacity for each grid-point. We compute monthly anomalies relative to a centered 31-year moving climatology. The results are insensitive to the residual linear trend.

2.2. Identification and Quantification of Heatwaves

We identify heatwaves during high summer (July and August, hereafter JA). For each land grid-point and calendar day, we use a percentile based heatwave definition (Perkins & Alexander, 2013). Heatwaves are defined when T2max exceeds the 90th percentile based on a centered 15-day, 31-year running window for at least three consecutive days. Hence, our heatwave definition considers spatial differences and temporal (both seasonal and long-term) variability of the threshold. A temporally fixed threshold would overestimate the identification of heatwaves during the climatological peak (i.e., August) and at the end of the historical run due to increasing temperatures driven by global warming.

The intensity of heatwaves is expressed as cumulative heat (Perkins-Kirkpatrick & Lewis, 2020). The cumulative heat is obtained by seasonal (JA) integration of heat exceeding the defined threshold during heatwave days. We additionally integrate the cumulative heat over the European domain (10°W–30°E, 35–60°N) after weighting each grid-point by the cosine of its latitude, obtaining a single value per year representing the intensity of EuSHWs. We evaluate the cumulative heat of 15,600 historical summers and select 10,000 years: 5,000 years with highest cumulative heat and 5,000 years with lowest cumulative heat. We consider these two sets as EuSHW years and non-EuSHW years, respectively.

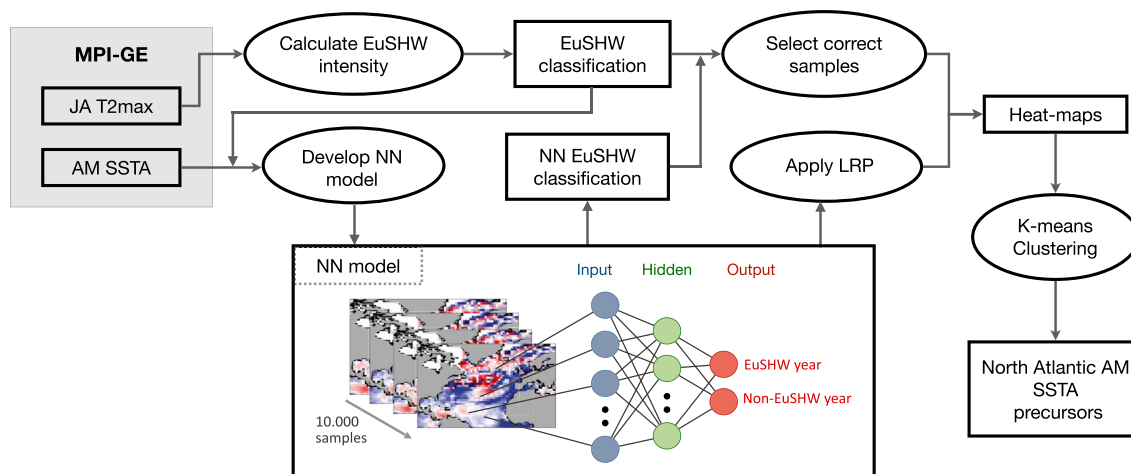


Figure 1. Schematic representation of the methodology employed here to identify North Atlantic spring (April and May; AM) sea surface temperature anomalies as a precursor of European summer (July and August; JA) heatwaves (EuSHWs) using neural-network (NN) based explainable artificial intelligence method, layerwise relevance propagation (LRP).

2.3. Neural-Network Set-Up

We develop a fully connected NN model (Lecun et al., 2015) for a supervised classification of the previously selected 10,000 years (Section 2.2) using spring (April and May, hereafter AM) mean North Atlantic (100°W – 30°E , 0 – 80°N) SSTAs (Figure 1). Our NN contains three layers. The first layer is the input layer, where we insert standardized AM North Atlantic SSTAs in a vectorized form (1,584 features). The second layer is the hidden layer and contains 20 neurons with rectified linear unit (Relu) activation function. We use L2 regularization with coefficient 2.0 to avoid overfitting. The third layer is the output layer and it has two neurons: one for EuSHW years and one for non-EuSHW years. We apply the softmax operator to obtain the probability of each sample belonging to the EuSHW and non-EuSHW years. The output neuron with highest probability determines the NN EuSHW classification. We train the model with 80% randomly shuffled samples and validate with the remaining 20%. A slightly different selection of hyperparameters and different methods of splitting the training and validation sets (i.e., splitting the time dimension in chunks of five consecutive years or splitting the ensemble dimension) do not influence the findings of this paper.

We evaluate the model performance by comparing the NN EuSHW classification to the EuSHW classification introduced in Section 2.2, and select the correctly classified samples. We use LRP to obtain one heat-map per correctly classified sample highlighting which grid-points from the input layer are most relevant to differentiate between EuSHW and non-EuSHW years. We use K-means (Hartigan & Wong, 1979) to cluster the LRP relevance patterns of correctly classified EuSHW years with model confidence above 60%, and to identify the most important North Atlantic SSTAs as a precursor of different EuSHWs (Mayer & Barnes, 2021). The results are insensitive to the selection of the confidence threshold.

3. Results

Our NN model correctly classifies 71% and 72% of EuSHW and non-EuSHW years: 3,567 and 3,598 samples, respectively. The performance is similar both in training and validation sets indicating that the model does not overfit. AM SSTA composites of correctly classified samples show that the tripolar North Atlantic pattern with opposite phases leads to EuSHW and non-EuSHW years (Figures 2a and 2c). Negative SSTAs in the SPG and the tropical Atlantic, and positive SSTAs in the Subtropical Gyre precede summers classified as EuSHW years (Figure 2a). In contrast, positive SSTAs in the SPG and tropical Atlantic, and negative SSTAs in the Subtropical Gyre precede summers classified as non-EuSHW years (Figure 2c).

Twenty-nine percent of EuSHW years that our model incorrectly classifies as non-EuSHW years, mainly the least intense EuSHW years (Figure S1 in Supporting Information S1), indicate that other processes besides North Atlantic SSTAs play a role in the development of EuSHWs. Weiland et al. (2021) demonstrated that the European summer atmospheric circulation depends on its early summer atmospheric state, which can persist for up to

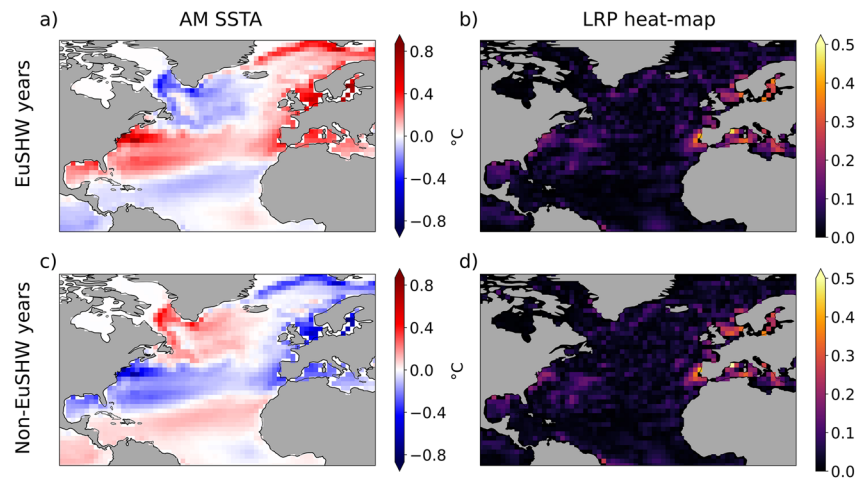


Figure 2. April and May (AM) mean SSTA composites of correctly classified; (a) European summer heatwave (EuSHW) years; (c) non-EuSHW years. Layerwise relevance propagation (LRP) heat-map composites of correctly classified; (b) EuSHW years; (d) non-EuSHW years. LRP composites are computed after normalizing each sample between 0 and 1.

45 days and could lead to a heatwave. In addition, Mecking et al. (2019) showed that matching atmospheric and sea-ice conditions were fundamental for the 2015 EuSHW.

In addition to the North Atlantic pattern, we find that positive and negative SSTAs surrounding the European continent also precede EuSHW years and non-EuSHW years (Figures 2a and 2c). The LRP heat-map composites of correctly classified samples highlight the European regional seas as the most important regions to differentiate EuSHW and non-EuSHW years (Figures 2b and 2d). We hypothesize that the heat-maps of correctly classified EuSHW years contain distinct patterns that highlight different regional SSTAs, and that different regional SSTAs are the precursor of different EuSHWs.

We obtain three LRP clusters all showing the tripolar North Atlantic pattern with consistent positive SSTAs in the Subtropical Gyre (Figures 3b, 3e and 3h), but highlighting different regional seas (Figures 3a, 3d and 3g). The first cluster highlights positive SSTAs west of the Iberian Peninsula and contains the strongest western EuSHWs (Figures 3a–3c). The second cluster highlights positive SSTAs in the Mediterranean Sea and contains the strongest southeastern EuSHWs (Figures 3d–3f). The third cluster highlights positive SSTAs in the North Sea and the Baltic Sea, and contains southeastern EuSHWs, although of less intensity than cluster 2 (Figures 3g–3i).

Our results suggest that, on the one hand, the tripolar North Atlantic pattern with negative SSTAs in SPG and western tropical Atlantic and positive SSTAs in the Subtropical Gyre is a precursor of EuSHWs, in agreement with Cassou et al. (2005), Duchez et al. (2016) and Wulff et al. (2017). However, the most consistent feature within the tripolar North Atlantic pattern preceding EuSHWs is the anomalously warm Subtropical Gyre. Disturbances in Subtropical North Atlantic SSTs and the respective diabatic heating anomalies are thought to be a source of Rossby waves which affect the European climate (Chen et al., 2020; Li & Ruan, 2018; Lim, 2015). On the other hand, the regional seas highlighted by the LRP heat-maps as the most relevant precursors for EuSHWs, appear to be the precursors of different types of EuSHWs.

The tripolar North Atlantic pattern, forced by winter atmospheric circulation anomalies, persists through spring and creates a reversed ocean-to-atmosphere forcing, preconditioning the occurrence of EuSHWs (Czaja & Frankignoul, 2002; Gastineau & Frankignoul, 2015; Ossó et al., 2018; Rodwell, 2002). In addition, we argue that positive regional SSTAs enhance the persistence of distinct blocking patterns and modulate spring precipitations and early summer SM anomalies in different European regions, preconditioning different types of EuSHWs. Although the SM can have a memory of several months (Hagemann & Stacke, 2015) and negative anomalies could be the product of the preceding dry winter, the soil dries considerably from early spring to early summer, consistent with our explanation (Figure S2 in Supporting Information S1).

Using the complete historical MPI-GE data set we linearly regress AM SSTAs averaged over the regional seas (boxes in Figures 3b, 3e and 3h) with AM Z500 anomalies, AM TP anomalies, June SM anomalies and JA cumulative heat anomalies on a grid-point level. Positive AM SSTAs west of the Iberian Peninsula relate to positive

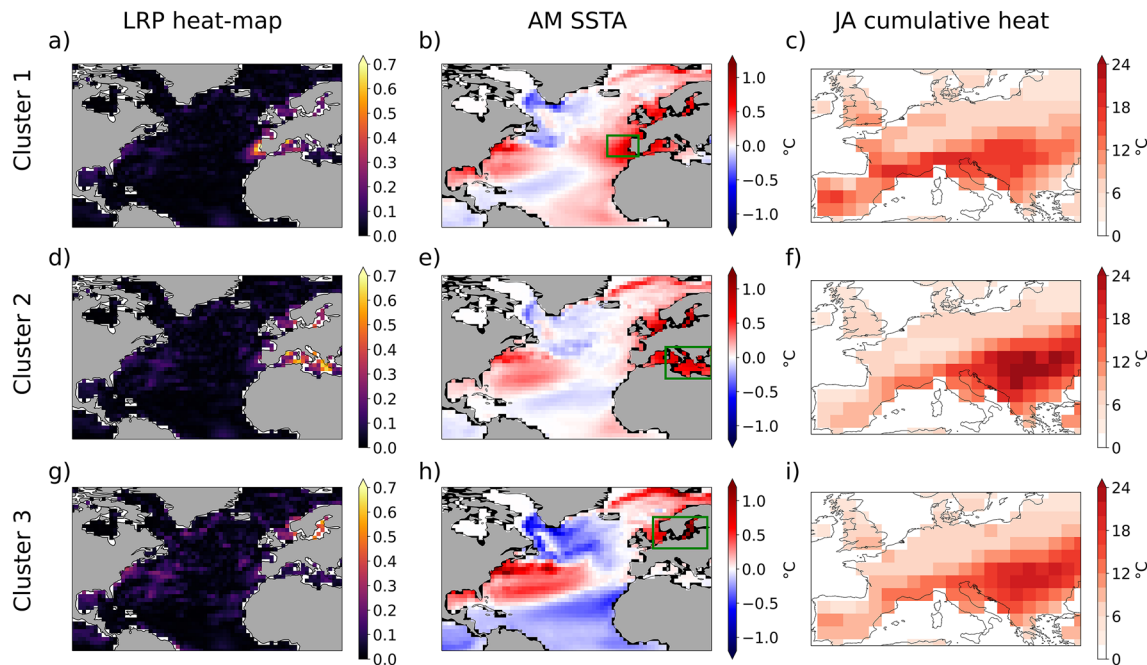


Figure 3. K-means clustering of layerwise relevance propagation (LRP) heat-maps for correctly classified European summer heatwave years with model confidence above 60%. Cluster composites of; (a, d, g) LRP heat-maps; (b, e, h) April and May mean SSTAs; (c, f, i) July and August heatwave intensity expressed as cumulative heat. Cluster one contains 1,103 samples, cluster two 814 samples and cluster three 903 samples.

AM Z500 anomalies, dry AM TP and June SM anomalies, and an increase of EuSHW intensity in western Europe (Figures 4a–4d). Positive AM SSTAs in the Mediterranean Sea relate to positive AM Z500 anomalies, dry AM TP and June SM anomalies, and an increase of EuSHW intensity in southeastern Europe (Figures 4e–4h). Positive AM SSTAs in the North Sea and the Baltic Sea relate to positive AM Z500 anomalies, dry AM TP and June SM anomalies, and an increase of EuSHW intensity in southeastern Europe (Figures 4i–4l).

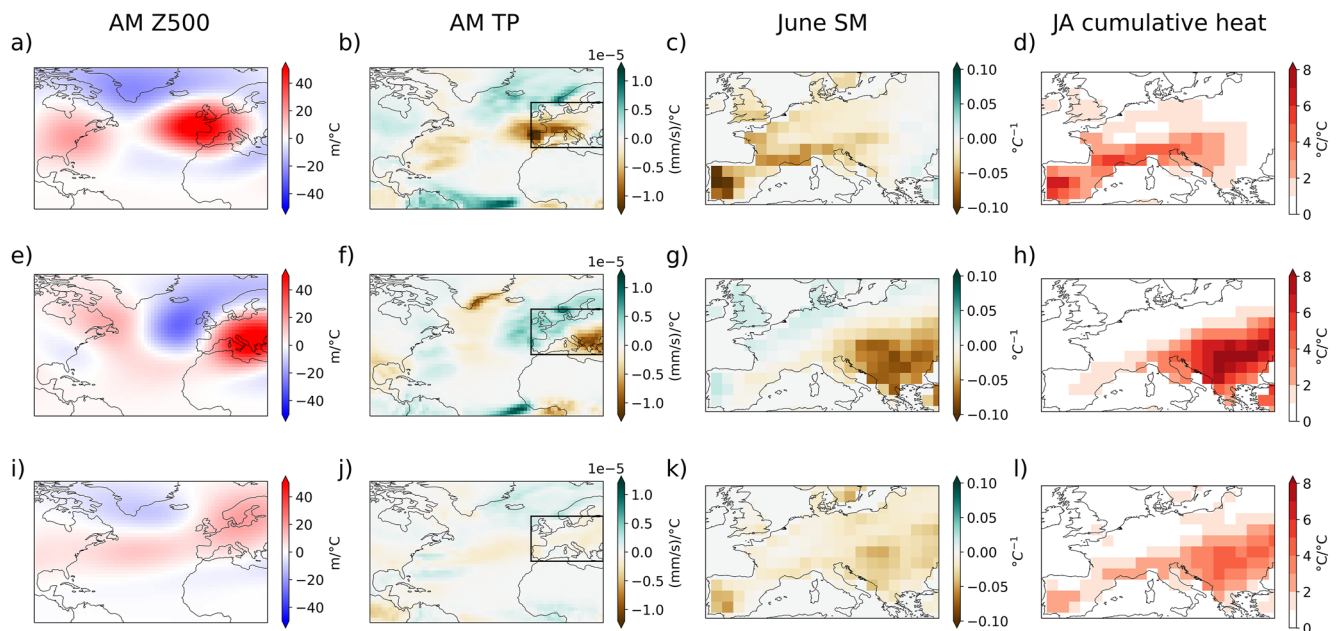


Figure 4. Linear regression coefficients for the entire historical MPI Grand-Ensemble data set between April and May (AM) mean sea surface temperature anomalies averaged over the boxes in Figures 3b, 3e and 3h and; (a, e, i) AM mean Z500 anomalies; (b, f, j) AM mean total precipitation anomalies; (c, g, k) June soil moisture anomalies; (d, h, l) July and August heatwave intensity anomalies expressed as cumulative heat.

The relationship between SSTAs in the North Sea and Baltic Sea and the intensity of southeastern EuSHWs (Figures 4i–4l) could be a combined effect of regional SSTAs and the winter NAO. Unlike positive SSTAs west of the Iberian Peninsula and in the Mediterranean Sea, positive SSTAs in the North Sea and Baltic Sea are related to the tripolar North Atlantic pattern (Figure S3 in Supporting Information S1), which is an imprint of the winter NAO (Czaja & Frankignoul, 2002). During the positive phase of NAO, the storm-track is shifted northward warming the North Sea and the Baltic Sea, drying the SM in southern Europe due to negative precipitation anomalies, and preconditioning southern EuSHWs (Wanner et al., 2001). However, positive SSTAs in the North Sea can directly enhance the occurrence of EuSHWs by reducing the meridional temperature gradient and baroclinic activity, allowing the persistence of high pressure systems over Europe (Feudale & Shukla, 2011).

Feudale and Shukla (2007, 2011) related the North Sea and the Mediterranean Sea to the 2003 EuSHW, which impacted western Europe. The 2003 EuSHW had several other contributing factors, including the northward displacement of the Azores high which relates to a deficit of precipitation in western Europe (Garcia-Herrera et al., 2010; Rashid et al., 2012). The northward displacement of Azores high could have been responsible for the strong deficit of SM in western Europe, and hence, for the westward location of the 2003 EuSHW. We find that the positive SSTAs west of the Iberian Peninsula are a precursor of western EuSHWs, and positive SSTAs in the North Sea and Mediterranean Sea are a precursor of southeastern EuSHWs, in agreement with Ionita et al. (2017) who showed that the warm Mediterranean Sea relates to dry and hot summer conditions in eastern Europe.

From our analysis, we are unable to conclude whether regional SSTAs play an active or passive role in the development of EuSHWs. We propose that positive regional SSTAs act as a heatwave amplification factor enhancing the persistence of blocking in different European regions. However, it is plausible that several episodes of blocking increase the regional SSTAs while reducing the SM. Future model experiments are required to disentangle the role of regional seas.

Our findings are only based on the MPI-GE data set, which contains model biases (Giorgetta et al., 2013; Hagemann et al., 2013; Müller et al., 2018). It has been shown that model wind biases can alter the propagation of Rossby waves induced by North Atlantic SSTAs (Li et al., 2021), which are relevant for modulating the atmospheric state and triggering heatwaves (Cassou et al., 2005; Kornhuber et al., 2020; Wulff et al., 2017). Although it has been demonstrated that the low resolution version of the MPI model represents well the connection between spring North Atlantic SSTA and Eurasian surface temperatures via atmospheric wave trains (Chen et al., 2021), the availability of other large ensembles with high temporal frequency and spatial resolution would aid to verify our results.

4. Conclusions

We investigate spring North Atlantic SSTAs as a precursor of EuSHWs combining the historical MPI-GE data set with NN based explainable artificial intelligence method, LRP. We identify the tripolar North Atlantic pattern with negative SSTAs in the SPG and the western tropical Atlantic as a precursor of EuSHWs. The most consistent feature of the tripolar pattern preceding EuSHWs is the positive SSTAs in the Subtropical Gyre. In addition, positive SSTAs in different regional seas emerge as the most robust precursors of different EuSHWs. While positive spring SSTAs west of the Iberian Peninsula precede western EuSHWs, positive spring SSTAs in the Mediterranean Sea, the North Sea and the Baltic Sea precede southeastern EuSHWs. The regional SSTAs can be related to distinct anticyclonic anomalies in spring, reducing the precipitation and leading to distinct patterns of negative SM anomalies in early summer. The patterns of SM anomalies resemble the location of the most intense EuSHWs. Here, we show that the combination of the spring tripolar North Atlantic pattern and regional SSTAs could aid in predicting the occurrence and location of EuSHWs.

Data Availability Statement

Data used in this study are available on the following website after registering at World Data Centre for Climate (<http://hdl.handle.net/21.14106/5a1b88c2bb1ae7736779602e6a201a119b7cf1bc>).

Acknowledgments

G.B.-A. is supported by the German Ministry of Education and Research (BMBF) under the ClimXtreme project NA2EE (Grant 01LP1902F). A.D. is supported by A4 (Aigéin, Aeráid, agus athrú Atlantaigh), funded by the Marine Institute (grant PBA/CC/18/01). E.A.B. is supported, in part, by the Regional and Global Model Analysis program area of the U.S. Department of Energy's Office of Biological and Environmental Research as part of the Program for Climate Model Diagnosis and Intercomparison project. We acknowledge the Deutsches Klimarechenzentrum (DKRZ) for the computational resources. We thank David Marcolino Nielsen for the insightful comments on the manuscript. We thank the two reviewers for their thoughtful comments.

References

Bach, S., Binder, A., Montavon, G., Klauschen, F., Müller, K. R., & Samek, W. (2015). On pixel-wise explanations for non-linear classifier decisions by layer-wise relevance propagation. *PLoS One*, *10*(7), 1–46. <https://doi.org/10.1371/journal.pone.0130140>

Bjerknes, J. (1964). Atlantic air-sea interaction. *Advances in Geophysics*, *10*, 1–82. [https://doi.org/10.1016/S0065-2687\(08\)60005-9](https://doi.org/10.1016/S0065-2687(08)60005-9)

Cassou, C., Terray, L., & Phillips, A. S. (2005). Tropical Atlantic influence on European heat waves. *Journal of Climate*, *18*(15), 2805–2811. <https://doi.org/10.1175/JCLI3506.1>

Chen, S., Wu, R., & Chen, W. (2021). Influence of North Atlantic sea surface temperature anomalies on springtime surface air temperature variation over Eurasia in CMIP5 models. *Climate Dynamics*, *57*(9–10), 2669–2686. <https://doi.org/10.1007/s00382-021-05826-5>

Chen, S., Wu, R., Chen, W., Hu, K., & Yu, B. (2020). Structure and dynamics of a springtime atmospheric wave train over the North Atlantic and Eurasia. *Climate Dynamics*, *54*(11–12), 5111–5126. <https://doi.org/10.1007/s00382-020-05274-7>

Czaja, A., & Frankignoul, C. (2002). Observed impact of Atlantic SST anomalies on the North Atlantic oscillation. *Journal of Climate*, *15*(18), 2707–2712. [https://doi.org/10.1175/1520-0442\(2002\)015<2707:OTRONA>2.0.CO;2](https://doi.org/10.1175/1520-0442(2002)015<2707:OTRONA>2.0.CO;2)

Duchez, A., Frajka-Williams, E., Josey, S. A., Evans, D. G., Grist, J. P., Marsh, R., et al. (2016). Drivers of exceptionally cold North Atlantic Ocean temperatures and their link to the 2015 European heat wave. *Environmental Research Letters*, *11*(7), 074004. <https://doi.org/10.1088/1748-9326/11/7/074004>

Feudale, L., & Shukla, J. (2007). Role of Mediterranean SST in enhancing the European heat wave of summer 2003. *Geophysical Research Letters*, *34*(3), 2–5. <https://doi.org/10.1029/2006GL027991>

Feudale, L., & Shukla, J. (2011). Influence of sea surface temperature on the European heat wave of 2003 summer. Part II: A modeling study. *Climate Dynamics*, *36*(9–10), 1705–1715. <https://doi.org/10.1007/s00382-010-0789-z>

Fischer, E. M., Seneviratne, S. I., Vidale, P. L., Lüthi, D., & Schär, C. (2007). Soil moisture-atmosphere interactions during the 2003 European summer heat wave. *Journal of Climate*, *20*(20), 5081–5099. <https://doi.org/10.1175/JCLI4288.1>

García-Herrera, R., Díaz, J., Trigo, R. M., Luterbacher, J., & Fischer, E. M. (2010). A review of the European summer heat wave of 2003. *Critical Reviews in Environmental Science and Technology*, *40*(4), 267–306. <https://doi.org/10.1080/10643380802238137>

Gastineau, G., & Frankignoul, C. (2015). Influence of the North Atlantic SST variability on the atmospheric circulation during the twentieth century. *Journal of Climate*, *28*(4), 1396–1416. <https://doi.org/10.1175/JCLI-D-14-00424.1>

Giorgetta, M. A., Jungclaus, J., Reick, C. H., Legutke, S., Bader, J., Böttinger, M., et al. (2013). Climate and carbon cycle changes from 1850 to 2100 in MPI-ESM simulations for the coupled model Intercomparison project phase 5. *Journal of Advances in Modeling Earth Systems*, *5*(3), 572–597. <https://doi.org/10.1002/jame.20038>

Hagemann, S., Loew, A., & Andersson, A. (2013). Combined evaluation of MPI-ESM land surface water and Energy fluxes. *Journal of Advances in Modeling Earth Systems*, *5*(2), 259–286. <https://doi.org/10.1029/2012MS000173>

Hagemann, S., & Stacke, T. (2015). Impact of the soil hydrology scheme on simulated soil moisture memory. *Climate Dynamics*, *44*(7–8), 1731–1750. <https://doi.org/10.1007/s00382-014-2221-6>

Hartigan, J. A., & Wong, M. A. (1979). A K-means clustering algorithm. *Journal of the Royal Statistical Society: Series C (Applied Statistics)*, *28*(1), 100–108.

Ionita, M., Tallaksen, L. M., Kingston, D. G., Stagge, J. H., Laaha, G., Van Lanen, H. A. J., et al. (2017). The European 2015 drought from a climatological perspective. *Hydrology and Earth System Sciences*, *21*(3), 1397–1419. <https://doi.org/10.5194/hess-21-1397-2017>

Kornhuber, K., Coumou, D., Vogel, E., Lesk, C., Donges, J. F., Lehmann, J., & Horton, R. M. (2020). Amplified Rossby waves enhance risk of concurrent heatwaves in major breadbasket regions. *Nature Climate Change*, *10*(1), 48–53. <https://doi.org/10.1038/s41558-019-0637-z>

Lecun, Y., Bengio, Y., & Hinton, G. (2015). Deep learning. *Nature*, *521*(7553), 436–444. <https://doi.org/10.1038/nature14539>

Li, J., & Ruan, C. (2018). The North Atlantic-Eurasian teleconnection in summer and its effects on Eurasian climates. *Environmental Research Letters*, *13*(2), 024007. <https://doi.org/10.1088/1748-9326/aa9d33>

Li, R. K. K., Tam, C. Y., Lau, N. C., Sohn, S. J., Ahn, J. B., & O'Reilly, C. (2021). Forcing mechanism of the silk road pattern and the sensitivity of Rossby-wave source hotspots to mean-state winds. *Quarterly Journal of the Royal Meteorological Society*, *147*(737), 2533–2546. <https://doi.org/10.1002/qj.4039>

Lim, Y. K. (2015). The East Atlantic/West Russia (EA/WR) teleconnection in the North Atlantic: Climate impact and relation to Rossby wave propagation. *Climate Dynamics*, *44*(11–12), 3211–3222. <https://doi.org/10.1007/s00382-014-2381-4>

Maher, N., Milinski, S., Suarez-Gutierrez, L., Botzet, M., Dobrynin, M., Kornbluh, L., et al. (2019). The Max Planck Institute Grand ensemble: Enabling the exploration of climate system variability. *Journal of Advances in Modeling Earth Systems*, *11*(7), 2050–2069. <https://doi.org/10.1029/2019MS001639>

Mayer, K. J., & Barnes, E. A. (2021). Subseasonal forecasts of opportunity identified by an explainable neural network. *Geophysical Research Letters*, *48*(10), 1–9. <https://doi.org/10.1029/2020GL092092>

Mecking, J. V., Drijfhout, S. S., Hirschi, J. J. M., & Blaker, A. T. (2019). Ocean and atmosphere influence on the 2015 European heatwave. *Environmental Research Letters*, *14*(11), 114035. <https://doi.org/10.1088/1748-9326/ab4d33>

Müller, W. A., Jungclaus, J. H., Mauritsen, T., Baehr, J., Bittner, M., Budich, R., et al. (2018). A higher-resolution version of the Max Planck Institute Earth System Model (MPI-ESM1.2-HR). *Journal of Advances in Modeling Earth Systems*, *10*(7), 1383–1413. <https://doi.org/10.1029/2017MS001217>

Ossó, A., Sutton, R., Shaffrey, L., & Dong, B. (2018). Observational Evidence of European Summer weather patterns predictable from spring. *Proceedings of the National Academy of Sciences of the United States of America*, *115*(1), 59–63. <https://doi.org/10.1073/pnas.1713146114>

Perkins, S. E., & Alexander, L. V. (2013). On the measurement of heat waves. *Journal of Climate*, *26*(13), 4500–4517. <https://doi.org/10.1175/JCLI-D-12-00383.1>

Perkins-Kirkpatrick, S. E., & Lewis, S. C. (2020). Increasing trends in regional heatwaves. *Nature Communications*, *11*(1), 1–8. <https://doi.org/10.1038/s41467-020-16970-7>

Rashid, S. A., Iqbal, M. J., & Hussain, M. A. (2012). Impact of North-South shift of Azores high on summer precipitation over North West Europe. *International Journal of Geosciences*, *03*(05), 992–999. <https://doi.org/10.4236/ijg.2012.325099>

Rex, D. F. (1950). Blocking action in the middle troposphere and its effect upon regional climate. *Tellus*, *2*(4), 275–301. <https://doi.org/10.3402/tellusa.v2i4.8603>

Rodwell, M. J. (2002). Atlantic Air-Sea interaction revisited. *International Geophysics*, *83*(C), 185–197. [https://doi.org/10.1016/S0074-6142\(02\)80167-X](https://doi.org/10.1016/S0074-6142(02)80167-X)

Seneviratne, S. I., Lüthi, D., Litschi, M., & Schär, C. (2006). Land-atmosphere coupling and climate change in Europe. *Nature*, *443*(7108), 205–209. <https://doi.org/10.1038/nature05095>

- Suarez-Gutierrez, L., Li, C., Müller, W. A., & Marotzke, J. (2018). Internal variability in European summer temperatures at 1.5°C and 2°C of global warming. *Environmental Research Letters*, *13*(6), 064026. <https://doi.org/10.1088/1748-9326/aaba58>
- Toms, B. A., Barnes, E. A., & Ebert-Uphoff, I. (2020). Physically interpretable neural networks for the Geosciences: Applications to Earth system variability. *Journal of Advances in Modeling Earth Systems*, *12*(9), 1–20. <https://doi.org/10.1029/2019MS002002>
- Treidl, R. A., Birch, E. C., & Sajecki, P. (1981). Blocking action in the Northern Hemisphere: A climatological study. *Atmosphere-Ocean*, *19*(1), 1–23. <https://doi.org/10.1080/07055900.1981.9649096>
- Wanner, H., Brönnimann, S., Casty, C., Gyalistras, D., Luterbacher, J., Schmutz, C., et al. (2001). North Atlantic Oscillation – Concepts and studies. *Surveys in Geophysics*, *22*(4), 321–382. <https://doi.org/10.1023/A:1014217317898>
- Watanabe, M., & Kimoto, M. (2000). Atmosphere-Ocean thermal coupling in the North Atlantic: A positive feedback. *Quarterly Journal of the Royal Meteorological Society*, *126*(570), 3343–3369. <https://doi.org/10.1256/smsqj.57016>
- Weiland, R. S., van der Wiel, K., Selten, F., & Coumou, D. (2021). Intransitive atmosphere dynamics leading to persistent hot-dry or cold-wet European summers. *Journal of Climate*, *34*(15), 6303–6317. <https://doi.org/10.1175/JCLI-D-20-0943.1>
- Wulff, C. O., Greatbatch, R. J., Domeisen, D. I. V., Gollan, G., & Hansen, F. (2017). Tropical forcing of the summer East Atlantic pattern. *Geophysical Research Letters*, *44*(21), 11166–11173. <https://doi.org/10.1002/2017GL075493>